



HAL
open science

Optimized Synthesis of 7-Azaindazole by a Diels–Alder Cascade and Associated Process Safety

Nicolas Brach, Vincent Le Foulher, Vincent Bizet, Marian Lanz, Fabrice Gallou, Corinne Bailly, Pascale Hoehn, Michael Parmentier, Nicolas Blanchard

► **To cite this version:**

Nicolas Brach, Vincent Le Foulher, Vincent Bizet, Marian Lanz, Fabrice Gallou, et al.. Optimized Synthesis of 7-Azaindazole by a Diels–Alder Cascade and Associated Process Safety. *Organic Process Research and Development*, 2020, 24 (5), pp.776-786. 10.1021/acs.oprd.0c00184 . hal-02991836

HAL Id: hal-02991836

<https://hal.science/hal-02991836>

Submitted on 6 Nov 2020

HAL is a multi-disciplinary open access archive for the deposit and dissemination of scientific research documents, whether they are published or not. The documents may come from teaching and research institutions in France or abroad, or from public or private research centers.

L'archive ouverte pluridisciplinaire **HAL**, est destinée au dépôt et à la diffusion de documents scientifiques de niveau recherche, publiés ou non, émanant des établissements d'enseignement et de recherche français ou étrangers, des laboratoires publics ou privés.

Optimized synthesis of 7-*aza*-indazole by Diels–Alder cascade and associated process safety

Nicolas Brach,[#] Vincent Le Foulher,[#] Vincent Bizet,[#] Marian Lanz,[‡] Fabrice Gallou,[‡] Corinne Bailly,[±] Pascale Hoehn,[‡] Michael Parmentier,^{‡*} Nicolas Blanchard^{#*}

[#] Université de Haute-Alsace, Université de Strasbourg, CNRS, LIMA, UMR 7042, 68000 Mulhouse, France

[‡] Chemical and Analytical Development, Novartis Pharma AG, CH-4056 Basel, Switzerland

[±] Service de Radiocristallographie, Fédération de Chimie Le Bel - FR2010, Université de Strasbourg, 1 rue Blaise Pascal, 67008 Strasbourg, France

Supporting Information Placeholder

ABSTRACT: Although pyrimidines are not among the most reactive partners in intramolecular inverse-electron demand $[4\pi_s+2\pi_s]$ reactions with alkynes, they could be activated under mild and practical conditions, leading to fused nitrogen-containing heterocycles. We report an optimized synthesis of a 5-iodo-7-*aza*-indazole by a one-pot Diels–Alder cascade that starts from a pyrimidine substituted in the 2-position by an (alkynyl)hydrazone. The safety of the process and the environmental impact were thoroughly evaluated. Eventually, a selection of cross-coupling reactions of **17** was studied and allowed the introduction of carbon- and nitrogen-based nucleophiles at the C5-position in good to excellent yields.

Keywords: cycloaddition, pyrimidine, *aza*-indazole, cascade, safety process, process mass intensity

Introduction

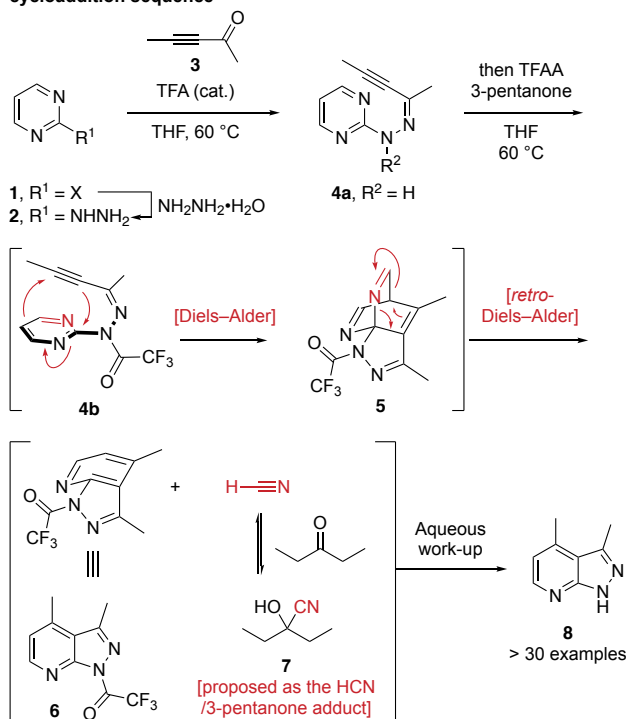
Diels–Alder cycloadditions between alkynes and pyrimidines are classified as inverse electron demand $[4\pi_s+2\pi_s]$ cycloadditions that lead to pyridines upon spontaneous *retro*-Diels–Alder reaction of the primary cycloadduct.^{1–5} Limitations of this conceptually interesting synthesis of pyridines are the high temperature (up to 280 °C under classical conditions⁶) and very long reaction times that are required^{7–9} to overcome the intrinsic lack of reactivity of these *aza*-dienes.^{10–19} On the other hand, we recently reported that pyrimidines substituted in the 2-position by an (alkynyl)hydrazone could be exceptionally activated towards intramolecular $[4\pi_s+2\pi_s]$ cycloadditions by a simple activation (Scheme 1, A).²⁰ In a practical one-pot procedure starting from 2-hydrazinopyrimidine **2**, it was shown that condensation with ynone **3** in the presence of catalytic amount of trifluoroacetic acid was rapid at 60 °C in THF, leading to hydrazone **4a**.

Upon *N*-trifluoroacetylation of hydrazone **4a**, **4b** is obtained which possesses a distorted conformation, perfectly organized for a $[4\pi_s+2\pi_s]$ cycloaddition leading to the primary cycloadduct **5**. The latter could not be detected and spontaneously undergoes a *retro*- $[4\pi_s+2\pi_s]$ delivering the *N*-trifluoroacetylated cycloadduct **6** and hydrogen cyanide. Extensive studies by Martin²¹ at Hoffmann-La Roche demonstrated that 3-pentanone was the most efficient trapping agent for HCN in such inverse electron demand Diels–Alder, likely via the formation of cyanohydrin **7** (although we were not able to detect **7** by ¹H NMR studies nor hydrogen cyanide by specific detector).²⁰ Upon aqueous work-up, 7-*aza*-indazole **8** is obtained as a single product of this Diels–Alder cascade. The reaction is general, and a wide functional group tolerance was observed.²⁰

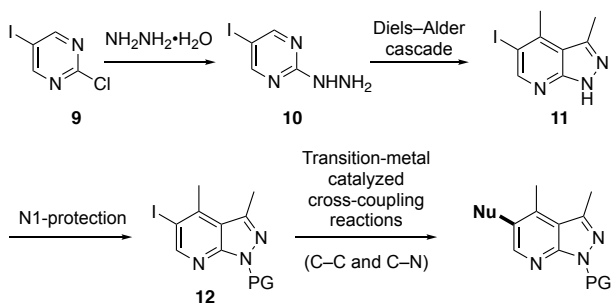
Having demonstrated the concept of pyrimidines activations towards $[4\pi_s+2\pi_s]$ cycloadditions under mild conditions, we focused on the optimization of the one-pot Diels–Alder sequence on a preparative scale (in terms of yields, ease of implementation and purification), on the safety of all the reactions at play, and also on cross-coupling reactions of a representative 5-iodo-7-*aza*-indazole for the synthesis of C–C and C–N bonds (Scheme 1, B). The results of these investigations are reported herein.

Scheme 1. Diels-Alder cycloadditions of pyrimidines under mild conditions.

A: 7-aza-indazoles by one-pot hydrazone formation/Diels-Alder cycloaddition sequence



B: This work: optimized one-pot procedure and selection of cross-coupling reactions of 12



- Optimized yields
- Thorough safety studies
- Ease of implementation
- Synthetic utility of 12 in cross-couplings
- Ease of purifications

Results and discussion

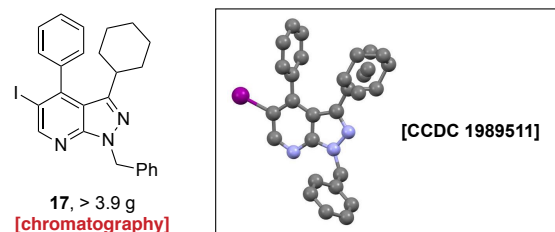
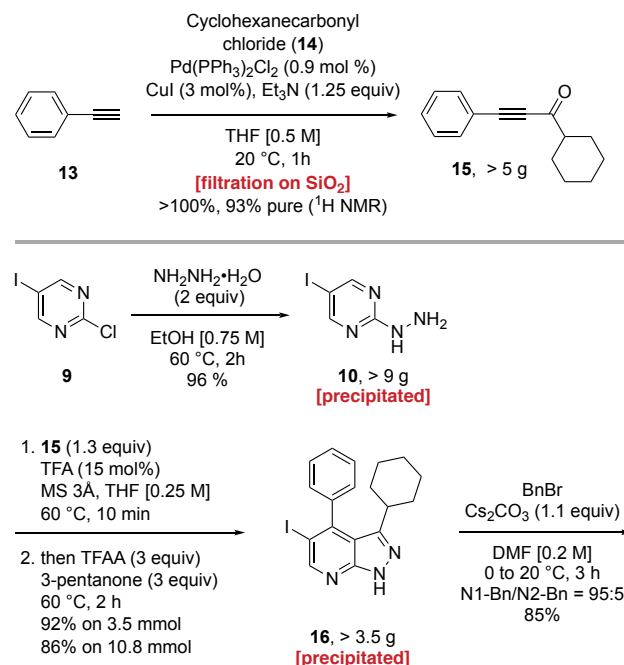
Synthesis of ynone 15. A first task was dedicated to the synthesis of a representative ynone, such as 1-cyclohexyl-3-phenylprop-2-yn-1-one **15** (Scheme 2). As reported by Cox,²² the Sonogashira cross-coupling between phenylacetylene **13** and cyclohexanecarbonyl chloride **14** in the presence of catalytic amounts of palladium(II) and copper(I) delivers **15** in excellent yields in 1 h at room temperature on more than 5 g in a single run. A simple filtration on a small pad of silica gel was found to be important to remove metallic traces that could be detrimental in the

next steps.²³⁻²⁵ Purity of ynone **15** was found to be 93% by ¹H NMR.^{26,27}

Synthesis of 2-hydrazinopyrimidine 10. We next focused on the synthesis of 2-hydrazinopyrimidine **10** by aromatic nucleophilic substitution of 2-chloro-5-iodopyrimidine **9**. This reaction occurred smoothly in ethanol (0.75 M) at 60 °C for 2 h. Upon cooling of the reaction mixture, **10** precipitated as grey powder that could be easily filtered. The reaction can be run on a preparative scale, and more than 9 g could be produced in a single run.

Optimization of the Diels-Alder/retro-Diels-Alder. Careful optimization of the Diels-Alder cascade demonstrated that condensation reaction between 2-hydrazino-5-iodo-pyrimidine **10** and ynone **15** (1.3 equivalent) was best conducted in the presence of trifluoroacetic acid (15 mol%) and 3 Å molecular sieves²⁸ in THF (0.25 M) at 60 °C for 10 min. Upon addition of trifluoroacetic anhydride (3 equivalents) and 3-pentanone (3 equivalents), heating of the solution at 60 °C was continued for 2 h.

Scheme 2. Optimization of the Diels-Alder cascade on gram-scale.



Aqueous work-up delivered *aza*-indazole **16** in 89±3% yield (92% on 3.5 mmol and 86% on 10.8 mmol) as a white solid, only slightly soluble in organic solvents. A simple filtration allows the recovery of the cycloadduct. While this procedure is simple and reliable on multigram scale, it should be kept in mind that the *retro*-Diels-Alder step is generating one equivalent of hydrogen cyanide (see also Scheme 1). Further optimizations are required on larger scales either to find more efficient trapping agents or finely tuned Diels-Alder precursors. As an example, a 4,6-dimethyl substituted pyrimidine core would lead to the elimination of acetonitrile in the *retro*-[4π_s+2π_s] cycloaddition, instead of hydrogen cyanide.

Cycloadduct **16** is next engaged in a benzylation reaction using benzyl bromide and cesium carbonate in DMF (0.2 M).²⁹ ¹H NMR of the crude reaction mixture showed that benzylation of N2 of 7-*aza*-indazole **16** occurs at 5% only (N1-Bn/N2-Bn = 95:5) and both compounds could be easily separated by chromatography on silica gel. Cycloadduct **17** was obtained in 85% yield as a white solid soluble in common organic solvents (toluene, tetrahydrofuran, dichloromethane, ethyl acetate...).

Figure 1. DSC analysis of compound 10

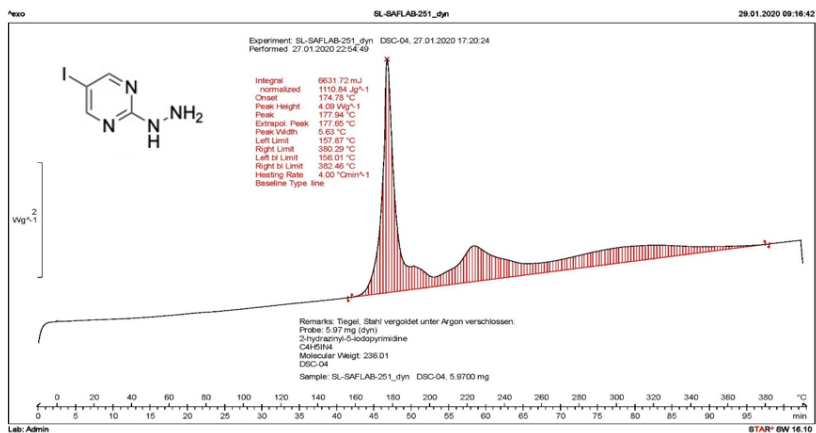


Figure 2. DSC analysis of phenylacetylene 13

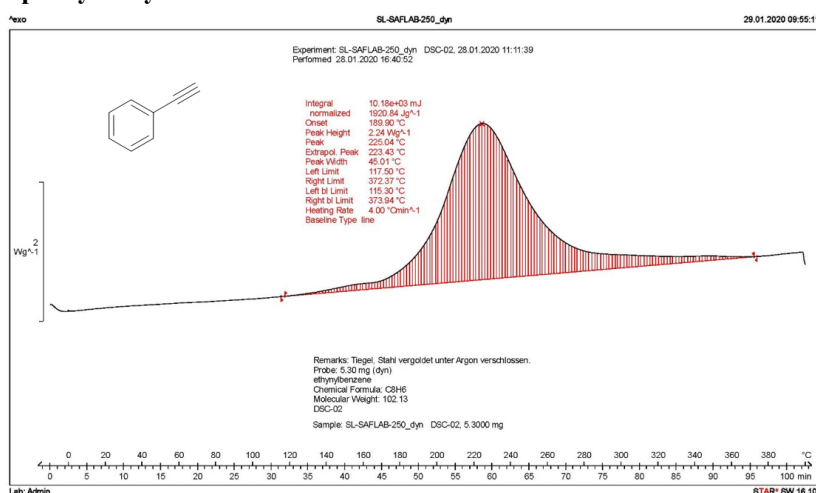
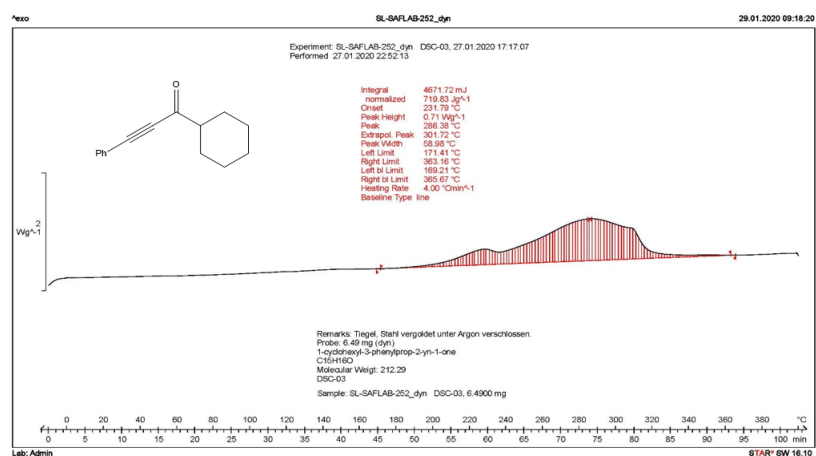


Figure 3. DSC analysis of 15



Single X-ray diffraction of 7-*aza*-indazole **17** (CCDC1989511, see Supporting Information) unambiguously proved the structure of this pericyclic cascade product. Overall, two precipitations and a single chromatography are required in this straightforward synthesis of a

complex 5-iodo-7-*aza*-indazole from a simple and inexpensive pyrimidine building block.

Process safety investigations.

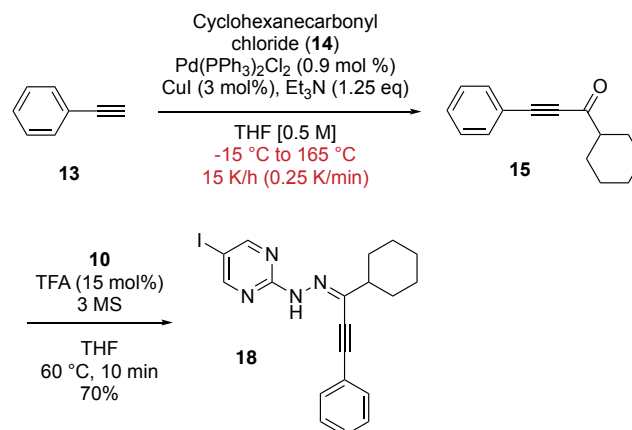
The process safety studies for the sequential steps were carried out with the major goal to design a safe process to support potential use on preparative scale. As our first step to explore the feasibility of applying this reaction on a pilot scale, we evaluated the thermal stability of all of the reagents and intermediates that are in sufficient concentrations under the reaction conditions using differential scanning calorimetry (DSC).

We first observed that the 2-chloro-5-iodopyrimidine **9** shows the onset of a very strong exothermal reaction starting above ca. 275 °C of at least -630 kJ/kg (see Supporting Information for DSC diagrams). Nevertheless, considering the reaction conditions used to produce **10** and the likelihood to reach such a high temperature, no specific measures needs to be implemented concerning its thermal stability. The use of hydrazine as reagent from an industrial manufacturing point of view is always safety relevant as hydrazine hydrate is a highly toxic, potentially carcinogenic, and corrosive liquid with a relatively low boiling point (120 °C).³⁰ In particular, the accumulation of this volatile reaction component in the headspace of a batch reactor can result in violent explosions. In accordance with literature data, the dilution of the system has a non-negligible impact on the flash point of hydrazine, compressibility and its potential deflagration. The current process is using hydrazine hydrate which is further diluted at 2 wt% with EtOH prior to be heated to 60 °C. This high dilution in addition to the moderate temperature ensure a process that can be safely operated.

The resulting product **10** has been submitted to DSC analysis and reveals an extremely strong exothermal reaction starting above ca. 155 °C (approx. -1111 kJ/kg) potentially leading to an adiabatic temperature increase of about 741 °C (Figure 1).³¹ The very high decomposition energy in compound **10**, lead us to further investigate its decomposition behavior. An isoDSC at 110 °C (reaction temp + 50 °C) over 12 h followed by a cooling step and a subsequent dynamic DSC run has been performed. It provided knowledge on potential decomposition behavior under the reaction temperature with sufficient safety margin. After ca. 460 min at 110 °C a very weak heat release is detected indicating a potential autocatalytic decomposition. In the determination test of the residual energy (after the isothermal measurement), the decomposition reaction is still registered. However, the overall energy is slightly lower than in the dynamic DSC test run on the fresh sample and the peak shape is substantially different. Moreover, the onset decomposition is shifted towards lower temperature (110 °C vs 155 °C). In light of these data, we concluded that the process to synthesize the compound **10** can be safely operated at the proposed temperature and that no specific measures needs to be implemented in regard to the thermal stability of all the starting materials neither the product used during this synthetic

step. Nevertheless, drying should be carefully controlled as it might be quality relevant (e.g. time and temperature) looking at the isothermal test combined with the determination of the residual heat release.

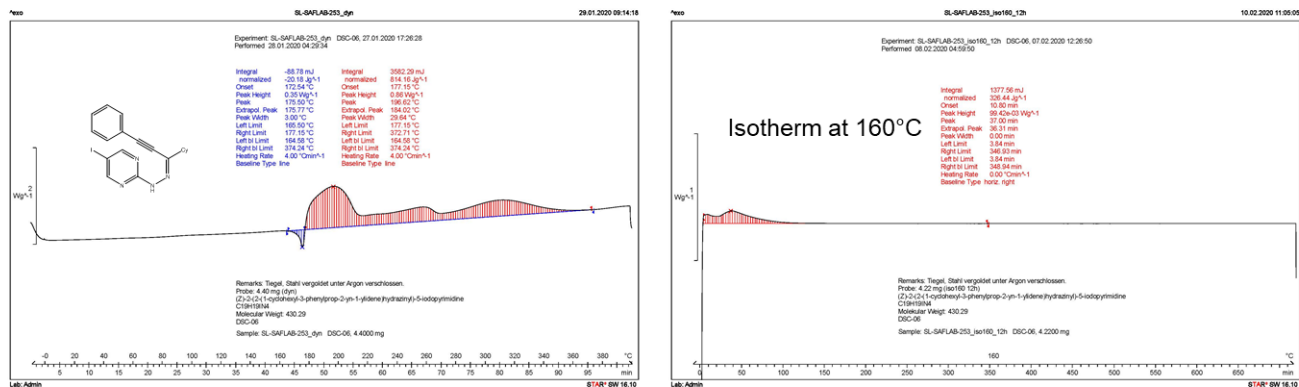
Scheme 3. Synthesis of **18**



The Sonogashira cross-coupling step to form **15** uses phenylacetylene as starting material. This commonly used starting material appears to be much less stable than expected; DSC analysis revealed its strong decomposition reaction starting at 115 °C: This highly exothermic event is characteristic of a violent decomposition ($\Delta H = -1921$ kJ/Kg) (Figure 2). The DSC measurement was conducted in a standard gold crucible and one could imagine that specific interaction between the compound and the crucible material can be responsible for this behavior. However, running the same experiment in a specific glass setup shows the same decomposition pattern.

In light of these results, we were then concerned about the potential impact of the palladium and copper catalyst used in the Sonogashira reaction (**13+14**→**15**, Schemes 2 and 3) and their potential influence on the onset of the decomposition. The dynamic SEDEX thermostability test of phenylacetylene **13**, in presence of the palladium and copper catalyst, shows no significant heat release up to 165 °C. The test was run on the reaction mixture (**13+14** with catalyst) and it shows a first moderate exothermal reaction starting above ca. 0 °C (approximately -60 kJ/kg, $\delta T_{\text{adiab}} = 40$ °C) most likely due to the reaction itself and a second one starting above ca. 115 °C (approximately -37 kJ/kg) that may corresponds to the beginning of the decomposition of the reaction product **15**. The isolated product **15** has a very high decomposition energy of -720 kJ/kg starting above 170 °C, making the process safely scalable considering the reaction conditions (reaction temperature = 25 °C).

Figure 4. DSC and isoDSC analysis of 18



The condensation of **10** and **15** followed by the Diels-Alder reaction leading to **16** is performed at 60 °C for a very short period. In order to study carefully the safety of the reaction, the stable hydrazone intermediate **18** has been prepared (Scheme 3) and submitted to DSC (Figure 4). As it can be envisioned considering its structure closely related to the hydrazine **10**, a substantial amount of energy can be released upon degradation (approx. -815 kJ/kg), starting at 175 °C after the melting of the compound. Nevertheless, no significant heat release could be observed when isoDSC was run at 110 °C (reaction temp + 50 °C). By increasing the temperature of the isoDSC measurement just below the endothermic point (160 °C), the onset of the decomposition could be observed but with a loss of energy of about 40%. Partial decomposition of the compound **18** can potentially explain this observation.

The final cycloadduct **16** resulting from the Diels-Alder cascade of the hydrazone intermediate **18** shows the onset of a moderate exothermic reaction starting above ca. 320 °C (approx. -153 kJ/kg) which is not of a concern regarding the very mild reaction conditions applied.

In conclusion, the thorough study of the sequential transformation of the pyrimidine **9** to the bicyclic cycloadduct **16** involving two highly energetic compound (namely phenylacetylene and hydrazine hydrate) can be safely operated using the described mild process. All the exotherms observed are well above the reaction temperature used during the process. Moreover, no significant onset shifts were observed due to the presence of catalysts.

Table 1. Calculated PMI for each step

Reaction	Reagents and substrates	Solvents	Water	PMI
13 → 15	2	24	55	82
9 → 10	1	8	2	12
10 → 16	5	14	49	68
16 → 17	2	39	16	57

Figure 5. Calculated PMI by step and cumulative

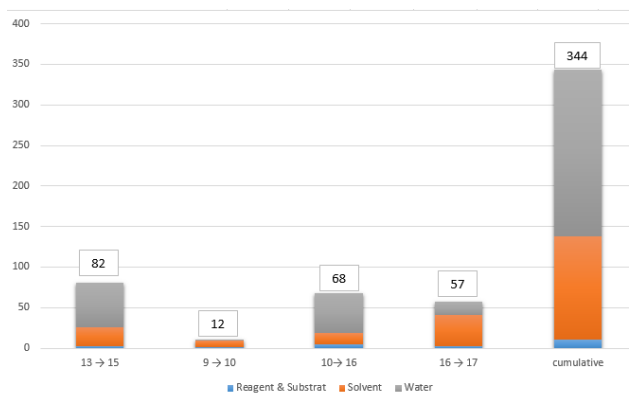
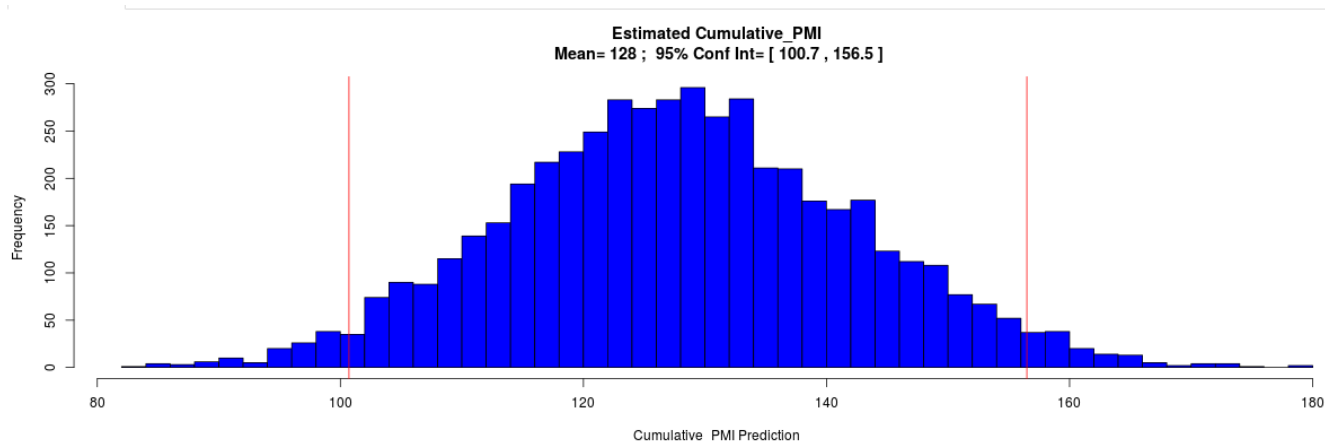


Figure 6. Estimated cumulative PMI



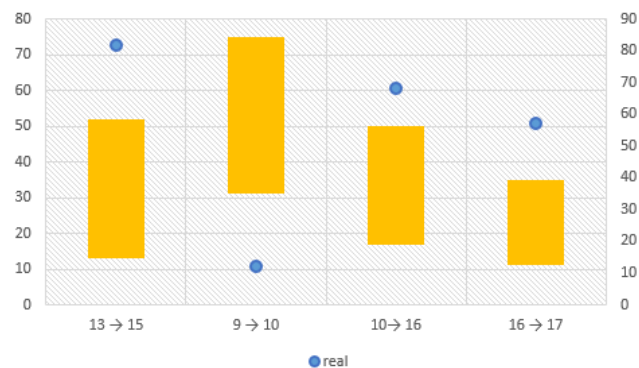
Environmental Impact Evaluation

While keeping in mind that the process to make the protected compound **17** is still at its research stage, we were interested to evaluate its environmental impact. Using a publicly available tool developed by the ACS Green Chemistry Institute Pharmaceutical Roundtable,³²⁻³⁴ we were able to calculate the overall waste generation to produce one mass unit of the final material **17** including organic solvent and aqueous waste (see Table 1, Figure 5 and detailed calculations in the Supporting Information). The Sonogashira cross-coupling step from **13** to **15** (see Scheme 2 for details) is based on a described process²² and was not fully optimized. Looking at generation of wastes, it can easily be seen that optimization of the aqueous workup will greatly improve the overall efficiency as two-third of the total mass accounts for water. This step represents by itself 45% of the total water consumption of the overall process and will be a topic to address over the future development. The aromatic nucleophilic substitution of **9** using hydrazine has a low PMI as the product **10** precipitated from the reaction mixture and requires only minimum washings to reach the targeted quality. The sequential Diels-Alder *retro*-Diels-Alder sequence (**10+15**→**16**, see Scheme 2 for details) has a good overall PMI of 68 as it combines two steps. The minimum amount of operations and washings make this step particularly efficient from a process point of view. Finally, the benzylation step (**16**→**17**)³⁵ was processed using standard literature protocol²⁹ and suffers the most from the use of DMF as organic solvent resulting by an increasing number of extractions during the downstream operations.

The cumulative PMI of 344 is not representative of the potential of such a streamlined and efficient synthetic

sequence. While scaling up each step, one can see opportunities for optimizing the solvent and/or water consumption. For the sake of comparison and to have a better idea on how far the process can be optimized in term of waste generation, we used the recently developed PMI prediction tool by Borovika *et al.* accessible online (Figures 6 and 7).³⁶⁻³⁸ The estimated cPMI range has a mean of 128 (see Supporting Information for details) with a 95% confidence interval. This is obviously below the value of 344 calculated with real data from the process. This theoretical cPMI value should be taken as a basis for future development opportunity as it represents an estimation of the waste generation of a given process for similar transformations, based on existing data from several pharmaceutical companies (at >1 kg scale).³⁹

Figure 7. Cumulative PMI for synthesis sequence up to compound **17 – predicted and actual values analyzed by the PMI Predictor tool.^a**

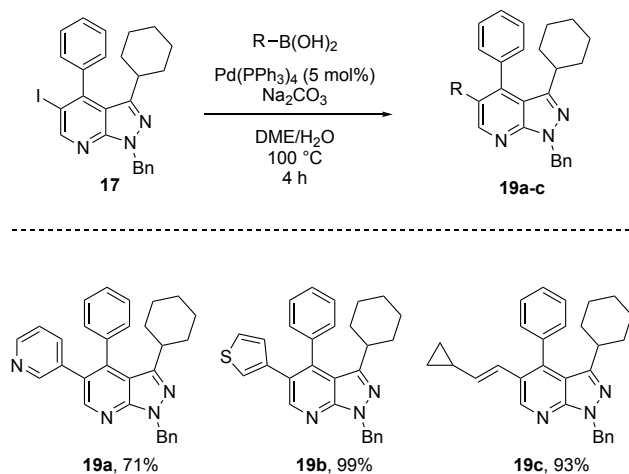


^a Blue circles denote the actual cumulative PMI for each intermediate in the synthetic route. Orange bars represent the predicted cPMI.

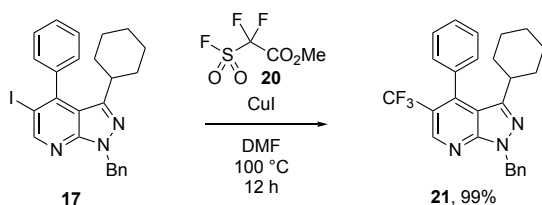
For example, optimization of the Sonogashira cross-coupling reaction can potentially lead to a significant gain of a minimum of 35% when reaching the high end of the typical range (**13**→**15**, Figure 7), while the *N*-benzylation can be reduced by 38% minimum (**16**→**17**, Figure 7). Future work upon scaling up will therefore focus on reducing the PMI of relevant steps.

Scheme 4. Arylation, vinylation and trifluoromethylation reactions of 7-*aza*-indazole **17**.

A: Palladium-catalyzed arylation and vinylation reactions



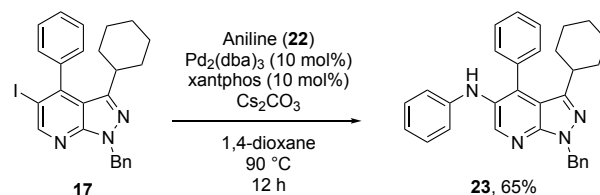
B: Copper-mediated trifluoromethylation reaction



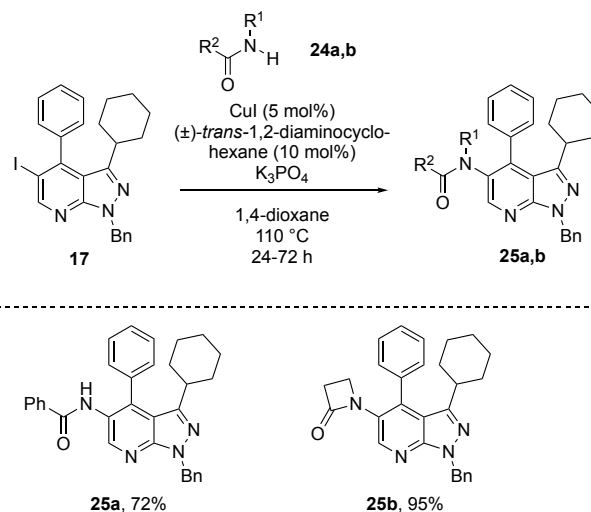
Cross-coupling reactions of cycloadduct **17 for the creation of C–C bonds.** Having at hand a scalable synthesis of 5-iodo-7-*aza*-indazole **17**, it was of interest to evaluate the late-stage diversification of this scaffold for the creation of C–C and C–N bonds on a limited number of examples. Arylation and vinylation reactions⁴⁰ of **17** were first investigated (Scheme 4, A), using three representative aryl- or vinylboronic acid, Pd(PPh₃)₄ (5 mol%) and sodium carbonate in a DME/H₂O (2:1) mixture at 100 °C for 4 h. 7-*Aza*-indazoles having a 5-(pyridin-3-yl), a 5-(thiophen-3-yl) or a 5-(cyclopropylvinyl) motif were obtained in good to excellent yields (**19a**, 71%; **19b**, 99%; **19c**, 93% respectively). Trifluoromethylation of **17** was also straightforward under Chen's copper(I)-mediated conditions^{41–43} (methyl fluorosulfonyldifluoroacetate **20**, DMF, 100 °C, 12 h). 5-Trifluoromethyl-7-*aza*-indazole **21** was obtained in quantitative yield (Scheme 4, B).

Scheme 5. Palladium-catalyzed and copper-mediated amination and amidation of 7-*aza*-indazole **17**.

A: Palladium-catalyzed amination reaction



B: Copper-catalyzed amidation reactions



Cross-coupling reactions of cycloadduct **17 for the creation of C–N bonds.** The formation of C–N bonds from **17** was also explored (Scheme 5). Aniline **22** could be efficiently cross-coupled to **17** using Pd₂(dba)₃ (10 mol%), xantphos (10 mol%), cesium carbonate in 1,4-dioxane at 90 °C for 12 h (Scheme 5, A).⁴⁴ Compound **23** was isolated in 65%. Introduction of amides and lactams was also evaluated under copper(I)-catalyzed cross-coupling conditions, with (±)-*trans*-1,2-diaminocyclohexane (10 mol%) as a ligand and potassium phosphate as a base in 1,4-dioxane at 110 °C (Scheme 5, B).⁴⁵ Benzamide **24a** and azetidinone **24b** were competent partners in these conditions and lead to **25a** (72%) and **25b** (95%) as the sole products.

Conclusions

Pyrimidines are simple building blocks that can be activated towards intramolecular [4π_s+2π_s] cycloadditions with alkynes under mild conditions. We have optimized the reaction conditions of a one-pot condensation/[4π_s+2π_s]/*retro*-[4π_s+2π_s] sequence that delivers 5-iodo-7-*aza*-indazole **16** in a straightforward manner, on a multigram scale. Extensive investigations of the safety of the process were conducted and the environmental impact

was evaluated. Eventually, diversification of 5-iodo-7-*aza*-indazole **17** was studied in a variety of transition-metal catalyzed cross-coupling reactions allowing the introduction of heteroaryl, vinyl, trifluoromethyl, aniline, amide and lactam in the C5-position with good to excellent yields. Synthetic strategies aiming at efficient disconnections in heterocyclic chemistry are a focus of many research groups. In this regard, pyrimidines are relevant (fused)pyridines precursors in terms of operational simplicity, process safety and diversification potential of the cycloadducts.

EXPERIMENTAL SECTION

General information. NMR spectra were recorded on Bruker AV 400 or AV 500 spectrometer at 400 MHz or 500 MHz for ^1H NMR, at 100 MHz or 125 MHz for ^{13}C NMR and at 471 MHz for ^{19}F . The spectra were calibrated using NMR solvent residual peaks as internal reference for ^1H NMR and ^{13}C NMR. Coupling constants (J) were reported in Hertz. Multiplicities are designed as singlet (s), doublet (d), triplet (t), quartet (q), quintuplet (quint), multiplet (m), broad (br) and possible combinations between them. Melting points were measured on a Heizank system Kofler Type WME (Wagne and Munz). High resolution mass spectra (HRMS) in positive modes were recorded using a 6520 series quadrupole time-of-flight (Q-TOF) mass spectrometer (Agilent) fitted with a multi-mode ion source (in mixed mode that enables both electrospray ionization, ESI, and atmospheric pressure chemical ionization, APCI). All sensitive reactions were carried out in oven-dried glassware under a nitrogen atmosphere using dry solvents, unless otherwise noted. Infrared spectra were recorded using a Spectrum Two FT-IR Spectrometer (PerkinElmer). THF was distilled under nitrogen from sodium-benzophenone; dichloromethane and 1,4-dioxane were distilled from calcium hydride. All other anhydrous solvents were purchased from Sigma-Aldrich. Molecular sieves were heated (either using a heat-gun or by flame-drying) under high vacuum just before use. Reagents were purchased from Merck, TCI, Fluorochem or Strem and used without further purification, unless otherwise noted. Concentration under reduced pressure was performed by rotary evaporation at appropriate temperature and pressure. Yields refer to chromatographically and spectroscopically (^1H , ^{13}C and ^{19}F NMR) homogenous materials, unless otherwise noted. Reactions were monitored by thin-layer chromatography (TLC) carried out on Merck TLC silica gel 60 F254 glass-coated plates, using UV light, potassium permanganate or vanillin (2-hydroxy-3-methoxybenzaldehyde) as visualizing agents. All separations were performed by column chromatography on Merck silica gel 60 (40–63 μm). DSC thermograms were recorded on Mettler Toledo DSC1, in high-pressure gold-plated DSC crucible closed under argon

atmosphere. SEDEX thermograms were recorded on SYSTAG TSC511 SEDEX in autoclave under stirring.

2-Hydrazinyl-5-iodo-pyrimidine (10). To a solution of 2-chloro-5-iodo-pyrimidine **9** (10 g, 41.6 mmol) in ethanol (55 mL, 0.75 M) was added hydrazine hydrate (4 mL, 83.2 mmol, 2 equiv.) at room temperature. The reaction mixture was heated at 60 °C for 2 h then cooled down to room temperature. The precipitate was filtered on a Büchner, rinsed with water (20 mL), ethanol (20 mL) and diethyl ether (20 mL) and dried under high vacuum until constant weight. 2-Hydrazinyl-5-iodo-pyrimidine **10** was obtained as a grey powder (9.38 g, 96 %). Spectroscopic data for 2-hydrazinyl-5-iodo-pyrimidine **10** are in agreement with reported data.⁴⁶ ^1H NMR (DMSO, 400 MHz, ppm) δ : 8.44 (s, 2H), 8.41 (s, 1H), 4.18 (s, 2H). ^{13}C NMR (DMSO, 100 MHz, ppm) δ : 162.5, 162.3, 76.0. IR (cm^{-1}) ν_{max} 1580, 1553, 1506, 1426, 1364, 1267, 1201, 1184, 1156, 1111, 988, 935, 852, 788, 643. Mp: 179 °C (lit. 196–197 °C after recrystallization from toluene).⁴⁶

1-Cyclohexyl-3-phenylprop-2-yn-1-one (15).²² To a solution of cyclohexanecarbonyl chloride (5 mL, 37.17 mmol) in THF (50 mL) under nitrogen were added successively phenylacetylene (2.72 mL, 24.78 mmol), Pd(PPh₃)₂Cl₂ (73 mg, 0.22 mmol, 0.9 mol%) and CuI (0.14 g, 0.74 mmol, 3 mol%). After 1 min, Et₃N (4.3 mL, 30.98 mmol) was added to the suspension and stirring was continued for 1 h at room temperature. The reaction mixture was diluted with diethyl ether (20 mL) and washed with water (50 mL). The combined organic phases were washed with a saturated aqueous solution of Na₂CO₃ (3x 75 mL), dried over MgSO₄, filtered and concentrated under vacuum. The residue was diluted in ethyl acetate (50 mL) and filtered through a pad of silica gel (approximately 3 cm height, 7 cm in diameter), eluting with ethyl acetate. The filtrate was concentrated under vacuum, offering 1-cyclohexyl-3-phenylprop-2-yn-1-one **15** as a dark red oil (5.44 g, >100 %, 93% pure by ^1H NMR) which was used without further purification. Spectroscopic data for 1-cyclohexyl-3-phenylprop-2-yn-1-one **15** are in agreement with reported data.²² ^1H NMR (CDCl₃, 400 MHz, ppm) δ : 7.59–7.57 (m, 2H), 7.44 (tt, J = 7.6, 1.5 Hz, 1H), 7.38 (2H, m, ArH), 2.55–2.47 (m, 1H), 2.08–2.03 (m, 2H), 1.81 (dt, J = 13.2, 3.9 Hz 2H), 1.71–1.66 (m, 1H), 1.57–1.45 (m, 2H), 1.39–1.10 (m, 3H). ^{13}C NMR (CDCl₃, 100 MHz, ppm) δ : 191.4, 133.0 (2C), 130.6, 128.6 (2C), 120.2, 91.3, 87.2, 52.3, 28.5 (2C), 25.8, 25.4 (2C).

3-Cyclohexyl-5-iodo-4-phenyl-1*H*-pyrazolo[3,4-*b*]pyridine (16). From **18**: To a solution of (*Z*)-2-(2-(1-cyclohexyl-3-phenylprop-2-yn-1-ylidene)hydrazinyl)-5-iodopyrimidine **18** (924 mg, 2.15 mmol) in THF (2.1 mL, 1 M) under nitrogen were added dropwise 3-pentanone (0.34 mL, 3.22 mmol, 1.5 equiv.) and trifluoroacetic anhydride (0.3 mL, 2.15 mmol, 1 equiv.). The reaction mixture was heated at 60 °C for 2 h, cooled down to room

temperature, diluted with ethyl acetate (3 mL) and washed with a saturated aqueous solution of Na₂CO₃ (3x 15 mL). The precipitate was filtered on a Büchner and washed with the minimum amount of ethyl acetate. 3-Cyclohexyl-5-iodo-4-phenyl-1*H*-pyrazolo[3,4-*b*]pyridine **16** was obtained as a white thin powder (822 mg, 94 %), sparingly soluble in DMSO. **One-pot synthesis from 10**: To a round bottom flask containing dry 3 Å molecular sieves (1 g) were successively added 2-hydrazinyl-5-iodo-pyrimidine **10** (0.86 g, 3.62 mmol), THF (14.5 mL, 0.25 M), 1-cyclohexyl-3-phenylprop-2-yn-1-one **15** (1 g, 4.71 mmol, 1.3 equiv.) and trifluoroacetic acid (0.04 mL, 0.54 mmol, 15 mol%) under nitrogen. The reaction mixture was heated at 60 °C for 10 min, then 3-pentanone (1.15 mL, 10.87 mmol, 3 equiv.) and trifluoroacetic anhydride (1.51 mL, 10.87 mmol, 3 equiv.) were added dropwise. The reaction mixture was heated at 60 °C for 2 h, cooled down to room temperature, concentrated under vacuum to half its volume, and diluted with ethyl acetate (5 mL). The resulting solution was washed with a saturated aqueous solution of Na₂CO₃ (3x 20 mL). The precipitate was filtered on a Büchner and washed with the minimum amount of ethyl acetate. 3-Cyclohexyl-5-iodo-4-phenyl-1*H*-pyrazolo[3,4-*b*]pyridine **16** was obtained as a white solid (1.34 g, 92 %). Starting from 2.57 g (10.87 mmol) of **10**, a slightly diminished yield was obtained (86%, 3.77 g of cycloadduct **16**). ¹H NMR (DMSO, 400 MHz, ppm) δ: 13.51 (s, 1H), 8.80 (s, 1H), 7.56 (m, 3H), 7.31-7.33 (m, 2H), 1.94-1.90 (m, 1H), 1.57-1.47 (m, 5H), 1.34-1.27 (m, 2H), 1.05 (m, 1H), 0.74-0.66 (m, 2H). ¹³C NMR (DMSO, 100 MHz, ppm) δ: 155.0, 152.0, 149.7, 148.8, 140.4, 129.1, 128.8 (2C), 128.7 (2C), 113.8, 90.1, 36.9, 32.8 (2C), 26.6 (2C), 25.9. IR (cm⁻¹) ν_{max}: 3180, 3127, 3010, 2926, 2847, 1585, 1446, 1282, 1196, 1172, 846, 756, 698, 6555. Mp: > 265 °C.

1-Benzyl-3-cyclohexyl-5-iodo-4-phenyl-1*H*-pyrazolo[3,4-*b*]pyridine (17). To a solution of 3-cyclohexyl-5-iodo-4-phenyl-1*H*-pyrazolo[3,4-*b*]pyridine **16** (1 g, 2.48 mmol) in DMF (12.4 mL, 0.2 M) under nitrogen were added Cs₂CO₃ (888.8 mg, 2.73 mmol) and benzyl bromide (0.33 mL, 2.73 mmol) at 0 °C. The reaction mixture was allowed to warm to room temperature and was stirred for 3 h, quenched with water (16 mL) then extracted with ethyl acetate (3x 15 mL). The combined organic phases were dried over MgSO₄, filtered then concentrated under vacuum. ¹H NMR (CDCl₃, 400 MHz) of the crude reaction mixture shows that 2 regioisomers were obtained in a N1/N2 ratio of 95:5, separable by flash chromatography on silica gel. The residue was purified by flash chromatography on silica gel (PE/AcOEt = 90:10 to 55:45). 1-Benzyl-3-cyclohexyl-5-iodo-4-phenyl-1*H*-pyrazolo[3,4-*b*]pyridine **17** was obtained as a white solid (1.03 g, 84 %). Upon scaling-up of this reaction on 3.77 g of **16**, 1-benzyl-3-cyclohexyl-5-iodo-4-phenyl-1*H*-pyrazolo[3,4-*b*]pyridine **17** was obtained in 85% yield (3.9 g). ¹H NMR (CDCl₃, 400 MHz, ppm) δ: 8.80 (s, 1H), 7.51 (m, 3H), 7.32-7.24 (m, 7H), 5.66 (s, 2H), 2.01-1.94 (m,

1H), 1.61-1.37 (m, 7H), 1.14-1.07 (m, 1H), 0.83-0.73 (m, 2H). ¹³C NMR (CDCl₃, 100 MHz, ppm) δ: 155.0, 150.1, 149.7, 149.0, 140.3, 137.2, 128.8, 128.5, (2C), 128.4, (2C), 128.3, (2C), 127.8 (2C), 127.5, 114.8, 89.5, 50.7, 36.9, 32.8 (2C), 26.5 (2C), 25.9. IR (cm⁻¹) ν_{max}: 3034, 2929, 2851, 1551, 1483, 1442, 1347, 1271, 1189, 1175, 767, 707, 693, 543. Mp: 159 °C.

(*Z*)-2-(2-(1-Cyclohexyl-3-phenylprop-2-yn-1-ylidene)hydrazinyl)-5-iodopyrimidine (18). To a Schlenk tube containing dry 3 Å molecular sieves (100 mg) were successively added 2-hydrazinyl-5-iodo-pyrimidine **10** (112.5 mg, 0.48 mmol), THF (2.4 mL, 0.2 M), 1-cyclohexyl-3-phenylprop-2-yn-1-one **15** (131.55 mg, 0.62 mmol) and trifluoroacetic acid (5 µL, 0.067 mmol, 15 mol%) under nitrogen. The reaction mixture was heated at 60 °C for 10 min, cooled down to room temperature and evaporated under vacuum. The residue was dissolved in dichloromethane (5 mL) and the solid was filtered on a Büchner. The solution was evaporated under vacuum, the resulting solid was triturated in acetone (10 mL) and filtered on a Büchner. (*Z*)-2-(2-(1-Cyclohexyl-3-phenylprop-2-yn-1-ylidene)hydrazinyl)-5-iodopyrimidine **18** was obtained as a white powder (142 mg, 70 %). ¹H NMR (CDCl₃, 400 MHz, ppm) δ: 9.12 (s, 1H), 8.60 (s, 2H), 7.60-7.57 (m, 2H), 7.44-7.38 (m, 3H), 2.70 (tt, *J* = 12.0, 3.6 Hz, 1H), 1.93-1.90 (m, 2H), 1.83-1.80 (m, 2H), 1.73-1.70 (m, 1H), 1.55 (qd, *J* = 12.4, 3.1 Hz, 2H), 1.40-1.20 (m, 3H). ¹³C NMR (CDCl₃, 100 MHz, ppm) δ: 163.5 (2C), 157.8, 140.4, 132.1 (2C), 129.9, 128.6, (2C), 120.9, 104.1, 79.7, 78.5, 44.7, 30.9 (2C), 25.8 (2C), 25.7. IR (cm⁻¹) ν_{max}: 3319, 2922, 2850, 1559, 1502, 1406, 1363, 1311, 1257, 1195, 1146, 1123, 1103, 992, 915, 782, 755, 742, 687, 639. Mp: 184 °C.

1-Benzyl-3-cyclohexyl-4-phenyl-5-(pyridin-3-yl)-1*H*-pyrazolo[3,4-*b*]pyridine (19a). To a solution of 1-benzyl-3-cyclohexyl-5-iodo-4-phenyl-1*H*-pyrazolo[3,4-*b*]pyridine **17** (50 mg, 0.1 mmol) in DME/H₂O (1:0.5 mL, 0.07 M) under nitrogen were added 3-pyridylboronic acid (14.9 mg, 0.12 mmol, 1.2 equiv.), Na₂CO₃ (12.9 mg, 0.12 mmol, 1.2 equiv.) and Pd(PPh₃)₄ (5.8 mg, 5 mol%). The reaction mixture was heated at 100 °C for 4 h, cooled down to room temperature and quenched with an aqueous solution of NaHCO₃ (10% in water, 3 mL). It was diluted in ethyl acetate (5mL) and filtered through a pad of silica gel. The pad was washed with EtOAc, and the filtrate washed with brine (5% in water). The organic phase was separated, dried over MgSO₄, filtered and evaporated under vacuum. The residue was purified by flash chromatography on silica gel (PE/AcOEt = 90:10). 1-Benzyl-3-cyclohexyl-4-phenyl-5-(pyridin-3-yl)-1*H*-pyrazolo[3,4-*b*]pyridine **19a** was obtained as a white solid (32 mg, 71 %). ¹H NMR (CDCl₃, 400 MHz, ppm) δ: 8.50 (s, 1H), 8.42 (dd, *J* = 4.7, 1.6 Hz, 2H), 7.40-7.37 (m, 3H), 7.34-7.30 (m, 5H), 7.27-7.26 (m, 1H), 7.20 (m, 2H), 7.13-7.11 (m, 1H), 5.74 (s, 2H), 2.23-2.19 (m, 1H), 1.62-1.58 (m,

4H), 1.51-1.42 (m, 3H), 1.15-1.11 (m, 1H), 0.88-0.77 (m, 2H). ^{13}C NMR (CDCl_3 , 100 MHz, ppm) δ : 150.8, 150.6, 150.5, 149.5, 147.8, 143.8, 137.5 (2C), 137.4, 135.9, 134.0, 129.5 (2C), 128.5 (2C), 128.2, 128.0 (2C), 127.8 (2C), 127.5, 125.9, 122.7, 112.7, 50.6, 37.1, 32.8 (2C), 26.6 (2C), 25.9. IR (cm^{-1}) ν_{max} : 3054, 3030, 2926, 2851, 1859, 1742, 1551, 1493, 1258, 1170, 1022, 712, 698, 647. Mp: 151 °C.

1-Benzyl-3-cyclohexyl-4-phenyl-5-(thiophen-3-yl)-1H-pyrazolo[3,4-*b*]pyridine (19b). To a solution of 1-benzyl-3-cyclohexyl-5-iodo-4-phenyl-1H-pyrazolo[3,4-*b*]pyridine **17** (50 mg, 0.1 mmol) in DME/ H_2O (1:0.5 mL, 0.07 M) under nitrogen were added 3-thiopheneboronic acid (15.5 mg, 0.12 mmol, 1.2 equiv.), Na_2CO_3 (12.9 mg, 0.12 mmol, 1.2 equiv.) and $\text{Pd}(\text{PPh}_3)_4$ (5.8 mg, 5 mol%). The reaction mixture was heated at 100 °C for 4 h, cooled down to room temperature and quenched with an aqueous solution of NaHCO_3 (10% in water, 3 mL). It was diluted in EtOAc (5 mL) and filtered through a pad of silica gel. The pad was washed with EtOAc, and the filtrate washed with brine (5% in water). The organic phase was separated, dried over MgSO_4 , filtered and evaporated under vacuum. The residue was purified by flash chromatography on silica gel (PE/AcOEt = 90:10). 1-Benzyl-3-cyclohexyl-4-phenyl-5-(thiophen-3-yl)-1H-pyrazolo[3,4-*b*]pyridine **19b** was obtained as a yellow solid (45 mg, 99 %). ^1H NMR (CDCl_3 , 400 MHz, ppm) δ : 8.62 (s, 1H), 7.39-7.35 (m, 5H), 7.32-7.29 (m, 2H), 7.26-7.23 (m, 3H), 7.13 (dd, $J = 5.0, 3.0$ Hz, 1H), 6.94 (dd, $J = 3.0, 1.3$ Hz, 1H), 6.75 (dd, $J = 5.0, 1.3$ Hz, 1H), 5.72 (s, 2H), 2.20-2.14 (m, 1H), 1.63-1.58 (m, 4H), 1.53-1.41 (m, 3H), 1.17-1.09 (m, 1H), 0.88-0.77 (m, 2H). ^{13}C NMR (CDCl_3 , 100 MHz, ppm) δ : 150.4, 150.3, 149.8, 142.8, 138.3, 137.6, 136.9, 129.2 (2C), 129.1 (2C), 128.5 (2C), 128.1, 128.0 (2C), 127.7 (2C), 127.4, 124.7, 124.3, 123.5, 112.8, 50.5, 37.05, 32.8 (2C), 26.6 (2C), 25.9. IR (cm^{-1}) ν_{max} : 3096, 3026, 2923, 2850, 1744, 1558, 1489, 1258, 1169, 784, 698, 666. Mp: 142 °C.

(E)-1-benzyl-3-cyclohexyl-5-(2-cyclopropylvinyl)-4-phenyl-1H-pyrazolo[3,4-*b*]pyridine (19c). To a solution of 1-benzyl-3-cyclohexyl-5-iodo-4-phenyl-1H-pyrazolo[3,4-*b*]pyridine **17** (50 mg, 0.1 mmol) in DME/ H_2O (1:0.5 mL, 0.07 M) under nitrogen were added 2-[(E)-2-cyclopropylethenyl]-4,4,5,5-tetramethyl-1,3,2-dioxaborolane (23.6 mg, 0.12 mmol, 1.2 equiv.), Na_2CO_3 (12.9 mg, 0.12 mmol, 1.2 equiv.) and $\text{Pd}(\text{PPh}_3)_4$ (5.8 mg, 5 mol%). The reaction mixture was heated at 100 °C for 4 h, cooled down to room temperature and quenched with an aqueous solution of NaHCO_3 (10% in water, 3 mL). It was diluted in EtOAc (5 mL) and filtered through a pad of silica gel. The pad was washed with EtOAc, and the filtrate washed with brine (5% in water). The organic phase was separated, dried over MgSO_4 , filtered and evaporated under vacuum. The residue was purified by flash chromatography on silica gel (PE/AcOEt = 90:10). (E)-1-Benzyl-3-cyclohexyl-5-(2-cyclopropylvinyl)-4-

phenyl-1H-pyrazolo[3,4-*b*]pyridine **19c** was obtained as a grey solid (41 mg, 93 %). ^1H NMR (CDCl_3 , 400 MHz, ppm) δ : 8.66 (s, 1H), 7.50-7.47 (m, 3H), 7.33-7.20 (m, 7H), 6.23 (d, $J = 16.0$ Hz, 1H), 5.67 (s, 2H), 5.58 (dd, $J = 16.0, 9.0$ Hz, 1H), 2.08-2.02 (m, 1H), 1.61-1.58 (m, 4H), 1.52-1.46 (m, 1H), 1.44-1.36 (m, 3H), 1.13-1.10 (m, 1H), 0.87-0.7 (m, 4H), 0.43-0.40 (m, 2H). ^{13}C NMR (CDCl_3 , 100 MHz, ppm) δ : 150.3, 150.0, 146.9, 141.3, 137.7, 136.6, 135.3, 129.1 (2C), 128.4 (2C), 128.1 (3C), 127.7 (2C), 127.3, 124.7, 122.8, 112.6, 50.4, 36.9, 32.8 (2C), 26.6 (2C), 25.9, 14.9, 7.30 (2C). IR (cm^{-1}) ν_{max} : 3003, 2928, 2846, 1645, 1573, 1493, 1257, 1045, 958, 706, 698, 648, 556. Mp: 144 °C.

1-Benzyl-3-cyclohexyl-4-phenyl-5-(trifluoromethyl)-1H-pyrazolo[3,4-*b*]pyridine (21). To a solution of 1-benzyl-3-cyclohexyl-5-iodo-4-phenyl-1H-pyrazolo[3,4-*b*]pyridine **17** (100 mg, 0.2 mmol) in DMF (0.9 mL, 0.23 M) under nitrogen were added CuI (57.9 mg, 0.3 mmol, 1.5 equiv.) and MFSDA (51 μL , 0.4 mmol, 2 equiv.). The flask was equipped with a bubbler and the reaction mixture was heated at 100 °C overnight. The solvent was removed under vacuum and the residue was purified by flash chromatography on silica gel (PE/AcOEt = 90:10). 1-Benzyl-3-cyclohexyl-4-phenyl-5-(trifluoromethyl)-1H-pyrazolo[3,4-*b*]pyridine **21** was obtained as a white solid (87 mg, 99 %). ^1H NMR (CDCl_3 , 400 MHz, ppm) δ : 8.81 (s, 1H), 7.54-7.45 (m, 3H), 7.38-7.28 (m, 7H), 5.70 (s, 2H), 1.87-1.80 (m, 1H), 1.62-1.38 (m, 7H), 1.15-1.07 (m, 1H), 0.81-0.71 (m, 2H). ^{13}C NMR (CDCl_3 , 100 MHz, ppm) δ : 151.7, 151.3, 145.9 (q, $J = 5.6$ Hz), 145.6, 137.0, 134.3, 128.8, 128.5 (2C), 128.4 (2C), 127.9 (2C), 127.7 (3C), 124.5 (q, $J = 273.8$ Hz), 117.6 (q, $J = 28.9$ Hz), 113.3, 50.7, 36.8, 32.8 (2C), 26.5 (2C), 25.8. ^{19}F NMR (CDCl_3 , 471 MHz, ppm) δ : - 54.5. IR (cm^{-1}) ν_{max} : 3034, 2932, 2850, 1887, 1577, 1563, 1323, 1279, 1204, 1120. Mp: 158 °C.

1-Benzyl-3-cyclohexyl-*N*,4-diphenyl-1H-pyrazolo[3,4-*b*]pyridin-5-amine (23). To a solution of 1-benzyl-3-cyclohexyl-5-iodo-4-phenyl-1H-pyrazolo[3,4-*b*]pyridine **17** (50 mg, 0.1 mmol) in 1,4-dioxane (0.5 mL, 0.2 M) under nitrogen were added aniline (14 μL , 0.15 mmol, 1.5 equiv.), Cs_2CO_3 (66 mg, 0.2 mmol, 2 equiv.), $\text{Pd}_2(\text{dba})_3$ (9.2 mg, 10 mol%) and xantphos (5.9 mg, 10 mol%). The reaction mixture was heated at 90 °C for 12 h. The mixture was diluted with EtOAc (5 mL), washed 3 times with water (10 mL), the organic phase was dried over MgSO_4 , filtered and the solvent removed under vacuum. The residue was purified by flash chromatography on silica gel (PE/AcOEt = 99:1). 1-Benzyl-3-cyclohexyl-*N*,4-diphenyl-1H-pyrazolo[3,4-*b*]pyridin-5-amine **23** was obtained as a dark oil (30 mg, 65 %). ^1H NMR (CDCl_3 , 400 MHz, ppm) δ : 8.60 (s, 1H), 7.48-7.46 (m, 3H), 7.40-7.35 (m, 6H), 7.27-7.25 (m, 1H), 7.19-7.15 (m, 2H), 6.83 (t, $J = 7.3$ Hz, 1H), 6.78 (d, $J = 8.1$ Hz, 2H), 5.70 (s, 2H), 5.13 (s, 1H), 2.21-2.14 (m, 1H), 1.63-1.61 (m, 4H), 1.54-1.41 (m, 3H), 1.17-1.09 (m, 1H), 0.87-0.77 (m, 2H). ^{13}C

NMR (CDCl₃, 100 MHz, ppm) δ : 149.4, 148.2, 146.2, 146.1, 137.7, 136.5, 134.3, 129.8, 129.4 (2C), 129.0 (2C), 128.7, 128.6 (2C), 128.5 (2C), 127.8 (2C), 127.4, 120.0, 115.5 (2C), 113.0, 50.5, 37.0, 32.8 (2C), 26.6 (2C), 25.9. IR (cm⁻¹) ν_{max} : 3400, 3030, 2927, 2851, 2245, 1731, 1600, 1495, 1270, 906, 727, 692.

***N*-(1-Benzyl-3-cyclohexyl-4-phenyl-1*H*-pyrazolo[3,4-*b*]pyridin-5-yl)benzamide (25a).** To a solution of 1-benzyl-3-cyclohexyl-5-iodo-4-phenyl-1*H*-pyrazolo[3,4-*b*]pyridine **17** (50 mg, 0.1 mmol) in 1,4-dioxane (1 mL, 0.1 M) under nitrogen were added benzamide (14.73 mg, 0.12 mmol, 1.2 equiv.), K₃PO₄ (43 mg, 0.2 mmol, 2 equiv.), CuI (1 mg, 5 mol%) and 1,2-cyclohexanediamine (1.2 μ L, 10 mol%). The reaction mixture was heated at 110 °C for 72 h. The mixture was diluted with EtOAc (5 mL), filtered through a pad of silica gel, the pad was then washed with EtOAc and the solvent was removed under vacuum. The residue was purified by flash chromatography on silica gel (PE/AcOEt = 65:35). *N*-(1-Benzyl-3-cyclohexyl-4-phenyl-1*H*-pyrazolo[3,4-*b*]pyridin-5-yl)benzamide **25a** was obtained as a white solid (35 mg, 72 %). ¹H NMR (CDCl₃, 400 MHz, ppm) δ : 9.30 (s, 1H), 7.58-7.54 (m, 5H), 7.49-7.45 (m, 2H), 7.46-7.41 (m, 2H), 7.39-7.35 (m, 4H), 7.32-7.28 (m, 2H), 7.26-7.22 (m, 1H), 5.72 (s, 2H), 2.19-2.12 (m, 1H), 1.63-1.41 (m, 7H), 1.16-1.08 (m, 1H), 0.86-0.76 (m, 2H). ¹³C NMR (CDCl₃, 100 MHz, ppm) δ : 165.9, 149.8, 148.7, 145.4, 137.5, 136.2, 134.2, 133.6, 131.9, 129.3, 129.0 (2C), 128.8 (2C), 128.7 (2C), 128.5 (2C), 127.7 (2C), 127.4, 126.9 (2C), 125.2, 112.2, 50.6, 37.0, 32.7 (2C), 26.5 (2C), 25.9. IR (cm⁻¹) ν_{max} : 3281, 3059, 2936, 2852, 1650, 1574, 1494, 1483, 1274, 863, 758, 704. Mp: 91 °C.

1-(1-Benzyl-3-cyclohexyl-4-phenyl-1*H*-pyrazolo[3,4-*b*]pyridin-5-yl)azetidin-2-one (25b). To a solution of 1-benzyl-3-cyclohexyl-5-iodo-4-phenyl-1*H*-pyrazolo[3,4-*b*]pyridine **17** (50 mg, 0.1 mmol) in 1,4-dioxane (1 mL, 0.1 M) under nitrogen were added azetidin-2-one (8.6 mg, 0.12 mmol, 1.2 equiv.), K₃PO₄ (43 mg, 0.2 mmol, 2 equiv.), CuI (1 mg, 5 mol%) and 1,2-cyclohexanediamine (1.2 μ L, 10 mol%). The reaction mixture was heated at 110 °C for 24 h. The mixture was diluted with EtOAc (5 mL), filtered through a pad of silica gel, the pad was then washed with EtOAc and the solvent was removed under vacuum. The residue was purified by flash chromatography on silica gel (PE/AcOEt = 65:35). 1-(1-Benzyl-3-cyclohexyl-4-phenyl-1*H*-pyrazolo[3,4-*b*]pyridin-5-yl)azetidin-2-one **25b** was obtained as a white solid (42 mg, 95 %). ¹H NMR (CDCl₃, 400 MHz, ppm) δ : 8.90 (s, 1H), 7.52-7.47 (m, 3H), 7.40-7.37 (m, 2H), 7.34-7.27 (m, 4H), 7.25-7.22 (m, 1H), 5.68 (s, 2H), 2.93-2.87 (m, 4H), 2.12-2.06 (m, 1H), 1.61-1.38 (m, 7H), 1.18-1.06 (m, 1H), 0.84-0.77 (m, 2H). ¹³C NMR (CDCl₃, 100 MHz, ppm) δ : 166.6, 150.2, 148.8, 145.6, 137.4, 137.2, 134.3, 129.0 (2C), 128.9, 128.4 (2C), 128.3 (2C), 127.8 (2C), 127.5, 126.1, 112.5, 50.6, 42.5, 37.2, 37.0, 32.7 (2C), 26.5

(2C), 25.9. IR (cm⁻¹) ν_{max} : 2922, 2846, 1742, 1570, 1511, 1490, 1371, 1271, 1146, 1048, 758, 699, 535. Mp: 95 °C.

ASSOCIATED CONTENT

Supporting Information. The Supporting Information is available free of charge on the ACS Publications website at DOI: 10.1021/....

DSC and SEDEX studies, PMI calculations, parameters for cPMI simulation, step yield vs step PMI estimation, X-ray crystallography data, copies of NMR spectra and references. Crystallographic data for the structure reported in this Article has been deposited at the Cambridge Crystallographic Data Centre under deposition number CCDC 1989511 (**17**, CIF).

AUTHOR INFORMATION

Corresponding Authors

M. Parmentier: michael.parmentier@novartis.com

N. Blanchard: n.blanchard@unistra.fr

ORCID

Nicolas Brach: 0000-0002-4416-6550

Vincent Bizet: 0000-0002-0870-1747

Fabrice Gallou: 0000-0001-8996-6079

Michael Parmentier: 0000-0002-1732-9641

Nicolas Blanchard: 0000-0002-3097-0548

Author Contributions

NBr and VLF optimized the synthetic chemistry part and analyzed data. PH, ML, FG and MP conducted the safety studies and analyzed data. CB solved the crystal structure. VB and NB designed and supervised the study. The manuscript was written through contributions of all authors. All authors have given approval to the final version of the manuscript.

Notes

The authors declare no competing financial interest.

ACKNOWLEDGMENTS

The authors acknowledge funding from the Université de Haute-Alsace, the Université de Strasbourg and the CNRS (NBR, VLF, VB, NBL).

REFERENCES

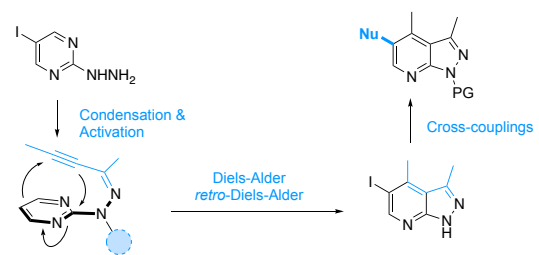
1. Ishihara, K.; Sakakura, A. in *Comprehensive Organic Synthesis II (Second Edition)* (ed Paul Knochel) 351-408 (Elsevier, 2014).
2. Ishihara, K.; Sakakura, A. in *Comprehensive Organic Synthesis II (Second Edition)* (ed Paul Knochel) 409-465 (Elsevier, 2014).
3. Boger, D. L. Diels-alder reactions of azadienes. *Tetrahedron* **1983**, *39*, 2869-2939.

4. Boger, D. L. Diels-Alder reactions of heterocyclic aza dienes. Scope and applications. *Chem. Rev.* **1986**, *86*, 781-793.
5. Foster, R. A. A.; Willis, M. C. Tandem inverse-electron-demand hetero-/retro-Diels-Alder reactions for aromatic nitrogen heterocycle synthesis. *Chem. Soc. Rev.* **2013**, *42*, 63-76.
6. Shao, B. Synthesis of fused bicyclic pyridines with microwave-assisted intramolecular hetero-Diels-Alder cycloaddition of acetylenic pyrimidines. *Tetrahedron Lett.* **2005**, *46*, 3423-3427.
7. Neunhoeffer, H.; Werner, G. Cycloadditionen mit Azabenzolen, VIII) Reaktion von Pyrimidinen mit *N,N*-Diäthyl-1-propinylamin. *Liebigs Ann. Chem.* **1974**, 1190-1194.
8. van der Plas, H. C. in *Advances in Heterocyclic Chemistry* Vol. Volume 84 (ed R. Katritzky Alan) 31-70 (Academic Press, 2003)
9. van der Plas, H. C. Thirty years of pyrimidine chemistry in the laboratory of organic chemistry at the Wageningen Agricultural University, The Netherlands (review). *Chem. Heterocycl. Compd.* **1994**, *30*, 1427-1443
10. Yang, Y.-F.; Liang, Y.; Liu, F.; Houk, K. N. Diels-Alder Reactivities of Benzene, Pyridine, and Di-, Tri-, and Tetrazines: The Roles of Geometrical Distortions and Orbital Interactions. *J. Am. Chem. Soc.* **2016**, *138*, 1660-1667.
11. Anderson, E. D.; Boger, D. L. Inverse Electron Demand Diels-Alder Reactions of 1,2,3-Triazines: Pronounced Substituent Effects on Reactivity and Cycloaddition Scope. *J. Am. Chem. Soc.* **2011**, *133*, 12285-12292.
12. Zhang, J.; Shukla, V.; Boger, D. L., Inverse Electron Demand Diels-Alder Reactions of Heterocyclic Azadienes, 1-Aza-1,3-Butadienes, Cyclopropanone Ketals, and Related Systems. A Retrospective. *J. Org. Chem.* **2019**, *84*, 9397-9445. Oliveira, B. L.; Guo, Z.; Bernardes, G. J. L. Inverse electron demand Diels-Alder reactions in chemical biology. *Chem. Soc. Rev.* **2017**, *46*, 4895-4950.
13. Liu, F.; Liang, Y.; Houk, K. N. Bioorthogonal Cycloadditions: Computational Analysis with the Distortion/Interaction Model and Predictions of Reactivities. *Acc. Chem. Res.* **2017**, *50*, 2297-2308.
14. Bickelhaupt, F. M.; Houk, K. N. Analyzing Reaction Rates with the Distortion/Interaction-Activation Strain Model. *Angew. Chem. Int. Ed.* **2017**, *56*, 10070-10086.
15. For a review, see: Duret, G.; Le Fouler, V.; Bissere, P.; Bizet, V.; Blanchard, N. Diels-Alder and Formal Diels-Alder Cycloaddition Reactions of Ynamines and Ynamides. *Eur. J. Org. Chem.* **2017**, 6816-6830.
16. Duret, G.; Quinlan, R.; Martin, R. E.; Bissere, P.; Neuburger, M.; Gandon, V.; Blanchard, N. Inverse Electron-Demand [4 + 2]-Cycloadditions of Ynamides: Access to Novel Pyridine Scaffolds. *Org. Lett.* **2016**, *18*, 1610-1613.
17. Duret, G.; Quinlan, R.; Yin, B.; Martin, R. E.; Bissere, P.; Neuburger, M.; Gandon, V.; Blanchard, N. Intramolecular Inverse Electron-Demand [4 + 2] Cycloadditions of Ynamides with Pyrimidines: Scope and Density Functional Theory Insights. *J. Org. Chem.* **2017**, *82*, 1726-1742.
18. Vermeeren, P.; van der Lubbe, S. C. C.; Fonseca Guerra, C.; Bickelhaupt, F. M.; Hamlin, T. A., Understanding chemical reactivity using the activation strain model. *Nature Protocols* **2020**, *15*, 649-667.
19. Grimblat, N.; Sarotti, A. M., Looking at the big picture in activation strain model/energy decomposition analysis: the case of the ortho-para regioselectivity rule in Diels-Alder reactions. *Org. Biomol. Chem.* **2020**, *18*, 1104-1111.
20. Le Fouler, V.; Chen, Y.; Gandon, V.; Bizet, V.; Salomé, C.; Fessard, T.; Liu, F.; Houk, K. N.; Blanchard, N., Activating Pyrimidines by Pre-distortion for the General Synthesis of 7-Aza-indazoles from 2-Hydrazonylpyrimidines via Intramolecular Diels-Alder Reactions. *J. Am. Chem. Soc.* **2019**, *141*, 15901-15909.
21. Martin, R. E.; Morawitz, F.; Kuratli, C.; Alker, A. M.; Alanine, A. I., Synthesis of Annulated Pyridines by Intramolecular Inverse-Electron-Demand Hetero-Diels-Alder Reaction under Superheated Continuous Flow Conditions. *Eur. J. Org. Chem.* **2012**, 47-52.
22. (a) Cox, R. J.; Ritson, D. J.; Dane, T. A.; Berge, J.; Charman, J. P. H.; Kantacha, A., Room temperature palladium catalysed coupling of acyl chlorides with terminal alkynes. *Chem. Commun.* **2005**, 1037-1039. For a review, see: (b) Nájera, C.; Sydnes, L. K.; Yus, M., Conjugated Ynones in Organic Synthesis. *Chem. Rev.* **2019**, *119*, 11110-11244.
23. It was observed that condensation of 2-hydrazinopyrimidine **10** with *unfiltered* ynone **15** leads to partial cyclization into pyrazole, a well-known process in heterocyclic chemistry. See references 24 and 25.
24. Bishop, B. C.; Brands, K. M. J.; Gibb, A. D.; Kennedy, D. J. Regioselective Synthesis of 1,3,5-Substituted Pyrazoles from Acetylenic Ketones and Hydrazines. *Synthesis* **2004**, 43-52.
25. Harigae, R.; Moriyama, K.; Togo, H. Preparation of 3,5-Disubstituted Pyrazoles and Isoxazoles from Terminal Alkynes, Aldehydes, Hydrazines, and Hydroxylamine. *J. Org. Chem.* **2014**, *79*, 2049-2058.
26. 1,4-Diphenyl-1,3-butadiyne was produced as a minor product in a Glaser-type homocoupling of phenylacetylene **13** and its presence was detected by ¹H NMR (non quantitative analysis, 10% by integration). For a review on Glaser reactions, see reference 27.
27. Evano, G.; Blanchard, N.; Toumi, M., Copper-Mediated Coupling Reactions and Their Applications in Natural Products and Designed Biomolecules Synthesis. *Chem. Rev.* **2008**, *108*, 3054-3131.
28. In the absence of molecular sieves, yields are in the 60% range. The role of this desiccant is to trap the water equivalent produced during the formation of hydrazone (**10**+**15** → **18**, Scheme 3) and thus to drive the equilibrium.
29. Clutterbuck, L. A.; Posada, C. G.; Visintin, C.; Riddall, D. R.; Lancaster, B.; Gane, P. J.; Garthwaite, J.; Selwood, D. L., Oxadiazolyindazole Sodium Channel Modulators are Neuroprotective toward Hippocampal Neurones. *J. Med. Chem.* **2009**, *52*, 2694-2707.
30. Niemeier, J. K.; Kjell, D. P., Hydrazine and Aqueous Hydrazine Solutions: Evaluating Safety in Chemical Processes. *Org. Proc. Res. Dev.* **2013**, *17*, 1580-1590.
31. Approximation for specific heat capacity for evaluation as: in average for all substances Cp = 1.5 kJ kg⁻¹ K⁻¹; First approximation for organic liquids: Cp = 1.8 kJ kg⁻¹ K⁻¹; First approximation for solids Cp = 1.3 kJ kg⁻¹ K⁻¹. Adapted from: Stoessel, F. in *Thermal Safety of Chemical Processes – Risk Assessment and Process Design*; Wiley-VCH Verlag GmbH & Co: 2008.
32. For Green Chemistry tools provided by ACS Green Chemistry, see: <https://www.acs.org/content/acs/en/greenchemistry/research-innovation/tools-for-green-chemistry.html>
33. Jimenez-Gonzalez, C.; Ponder, C. S.; Broxterman, Q. B.; Manley, J. B., Using the Right Green Yardstick: Why Process Mass Intensity Is Used in the Pharmaceutical Industry To Drive More Sustainable Processes. *Org. Proc. Res. Dev.* **2011**, *15*, 912-917.
34. Andraos, J. Relationships between step and cumulative PMI and E-factors: Implications on estimating material efficiency with respect to charting synthesis optimization strategies. *Green Processing and Synth.* **2019**, *8*, 324-336.
35. Solvents from silica gel chromatography were not included in the PMI calculation as a crystallization process can be potentially developed. Taken into account chromatography solvents would not show the real potential of the process, and only solvents, raw material and reagents of this reaction have been taken into account in the calculated PMIs. We thank a referee for bringing this point to the discussion.

36. Borovika, A.; Albrecht, J.; Li, J.; Wells, A. S.; Briddell, C.; Dillon, B. R.; Diorazio, L. J.; Gage, J. R.; Gallou, F.; Koenig, S. G.; Kopach, M. E.; Leahy, D. K.; Martinez, I.; Olbrich, M.; Piper, J. L.; Roschangar, F.; Sherer, E. C.; Eastgate, M. D., The PMI Predictor app to enable green-by-design chemical synthesis. *Nature Sustain.* **2019**, *2*, 1034-1040.
37. For PMI predictor tool, see: https://acsgcipc-pre-dictpmi.shinyapps.io/pmi_calculator/
38. Li, J.; Albrecht, J.; Borovika, A.; Eastgate, M. D., Evolving Green Chemistry Metrics into Predictive Tools for Decision Making and Benchmarking Analytics. *ACS Sustainable Chem. Eng.* **2018**, *6*, 1121-1132.
39. Li, J.; Simmons, E. M.; Eastgate, M. D., A data-driven strategy for predicting greenness scores, rationally comparing synthetic routes and benchmarking PMI outcomes for the synthesis of molecules in the pharmaceutical industry. *Green Chem.* **2017**, *19*, 127-139.
40. Uno, T.; Kawai, Y.; Yamashita, S.; Oshiumi, H.; Yoshimura, C.; Mizutani, T.; Suzuki, T.; Chong, K. T.; Shigeno, K.; Ohkubo, M.; Kodama, Y.; Muraoka, H.; Funabashi, K.; Takahashi, K.; Ohkubo, S.; Kitade, M., Discovery of 3-Ethyl-4-(3-isopropyl-4-(4-(1-methyl-1H-pyrazol-4-yl)-1H-imidazol-1-yl)-1H-pyrazolo[3,4-b]pyridin-1-yl)benzamide (TAS-116) as a Potent, Selective, and Orally Available HSP90 Inhibitor. *J. Med. Chem.* **2019**, *62*, 531-551.
41. Chen, Q.-Y.; Wu, S.-W., Methyl fluorosulphonyldifluoroacetate; a new trifluoromethylating agent. *J. Chem. Soc., Chem. Commun.* **1989**, 705-706.
42. Clarke, S. L.; McGlacken, G. P., Methyl fluorosulphonyldifluoroacetate (MFSDA): An Underutilised Reagent for Trifluoromethylation. *Chem. Eur. J.* **2017**, *23*, 1219-1230.
43. Hamilton, G. L.; Chen, H.; Deshmukh, G.; Eigenbrot, C.; Fong, R.; Johnson, A.; Kohli, P. B.; Lupardus, P. J.; Liederer, B. M.; Ramaswamy, S.; Wang, H.; Wang, J.; Xu, Z.; Zhu, Y.; Vucic, D.; Patel, S., Potent and selective inhibitors of receptor-interacting protein kinase 1 that lack an aromatic back pocket group. *Bioorg. Med. Chem. Lett.* **2019**, *29*, 1497-1501.
44. Zhang, J.; Xu, W.; Jian, S. Heterocyclic compounds as ERK inhibitors and their preparation. WO 2016026078 A1.
45. Klapars, A.; Huang, X.; Buchwald, S. L., A General and Efficient Copper Catalyst for the Amidation of Aryl Halides. *J. Am. Chem. Soc.* **2002**, *124*, 7421-7428.
46. Allen, D. W.; Buckland, D. J.; Hutley, B. G.; Oades, A. C.; Turner, J. B., Photolysis of 5-iodopyrimidines in benzene or heteroarenes; a convenient route to 5-phenyl- and 5-heteroaryl-pyrimidines. *J. Chem. Soc., Perkin Trans. 1* **1977**, 621-624.

Table of Contents graphic

Max: 8.5 cm x 4.75 cm



- Optimized sequence
 - Process safety
 - Diversity-oriented cross-couplings
 - Environmental impact
-